Noise Reduction Algorithm for Mobile LiDAR Data of Sand Ripples in Intertidal Zones of Beaches

Alain DE WULF, Michiel DECOCK, Annelies VANDENBULCKE, Cornelis STAL and Philippe DE MAEYER, Belgium.

Key words: Laser Scanning, Mobile Mapping, Intertidal Zones, Micro-Relief, Noise Filtering

SUMMARY

For the interdisciplinary research project *SeArch*, which aims at documenting the archaeological patrimony in the Belgian North Sea, some intertidal zones near Ostend (Belgium) were scanned using a kinematic platform. For a geometric reconstruction of beaches, one could also apply a static scanning method. Although this kind of mapping results in very precise data, scanning by means of a mobile platform significantly reduces the data acquisition time. A Terrestrial Laser Scanner (TLS), a Real-Time Kinematic Global Navigation Satellite System (RTK GNSS) and an Inertial Measurement Unit (IMU) were placed on a special service vehicle. The intensity of the laser beam, which reflects on the sand, as well as the derived geometry, was used to map the beach's micro-relief. Such a map revealing very small height differences offers the possibility to detect morphological characteristics of sand transport and the possible presence of archaeological structures beneath the beach surface.

A side effect of data acquisition using a laser scanner is the inclusion of noise in the point cloud. In this paper, an algorithm on the filtering of mobile LiDAR data on beach strip measurements in the intertidal zone will be discussed. This noise removal algorithm has to be performed in an efficient, non-time consuming and precise way. The filtering is based on statistical analysis of the echo backscatter and the geometric characteristics of the measured point. The presented noise reduction procedure appeared very effective for both the noise elimination as for the extraction of the micro-relief features.

Noise Reduction Algorithm for Mobile LiDAR Data of Sand Ripples in Intertidal Zones of Beaches

Alain DE WULF, Michiel DECOCK, Annelies VANDENBULCKE, Cornelis STAL and Philippe DE MAEYER, Belgium.

1. INTRODUCTION

Mapping the morphology of sandy beach offers interesting insights into aeolian sand transport. Besides, micro-ripples on the surface can indicate sub-surface archaeological relicts. In the context of a Belgian scientific interdisciplinary research project Search (Archaeological heritage in the North Sea, www.sea-arch.be) an analysis of the micro topography of the intertidal zones of selected beaches was required. The selected test zone was located at Raversijde, in the middle of the Belgian coastal area (fig. 1.1). The SeArch project aims to document and manage archaeological patrimony in the North Sea. DSMs are an indispensable tool for the development and sustainable management of cultural heritage and archaeological relicts. These 3D-models are commonly used for the analysis of existing archaeological features or for the detection of new features.

Initially, Airborne Laser Scanning (ALS) and Airborne Laser Bathymetry (ALB) seemed to be the most appropriate acquisition techniques for the shallow water detection (White, et al., 2011) (Middleton, et al., 2013). However, the Belgian coast environment is a challenging one. First, the turbidity of the North Sea is very high (the secchi depth is very limited, excluding ALB). Second, the weather conditions are rough (strong wind, frequent rain fall), causing frequent changes of the sand beach surface, requiring frequent measurements. An ALS or ALB techniques are therefore not preferred in such an environment. New surveying approaches were required. Previous feasibility studies have demonstrated that a mobile laser-scanning set-up is very promising for intertidal surface modelling in comparison with other measurement techniques (De Wulf, et al., 2014)

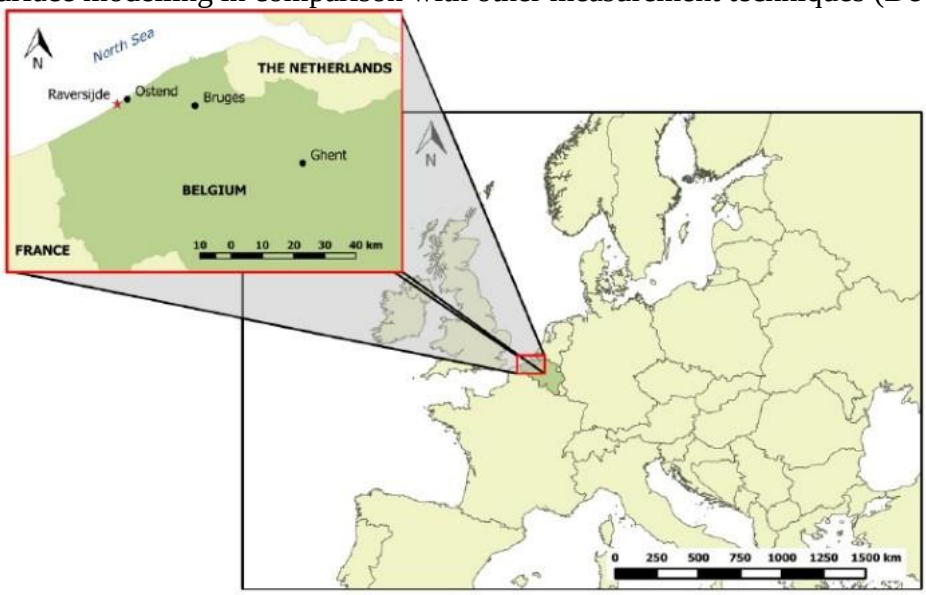

.
Figure 1.1: Geographic location of Belgium in Europe with detail map focussed on the survey region of Raversijde.

The same scanning platform is also used in the recently started Belgian scientific research project "CREST" (http://www.vliz.be/en/news?p=show&id=4402). Since the yearly volumes of sand for beach nourishments was increased, it is important to estimate aeolian sand transport to assess the artificial coastal safety by beach elevation and beach nourishment. As a result of storms, tourism, etc., a clear variation in morphology can be observed. Therefore, it is crucial to detect the variation in morphology of the intertidal zone and the rest of the sandy beach in time. Digital Surface Models (DSMs) are an indispensable data source for the management of coastal safety by beach elevation and beach nourishment. Unfortunately, coastal modelling suffers heavily from data gaps between land and shallow waters. It can be shown that onshore acquisition techniques may be adapted in order to fill the gap. In the framework of CREST, high resolution topography surveys will be carried out before and after storms and during experiments related to aeolian sand transport. Detailed morphological modelling using a prototype mobile platform (UTV, Special Service Vehicle) requires measurements with centimeter accuracy before and after major storm events. These measurements will be carried out for two test zones with a coastal stretch of about 500 meter length.

2. MOBILE SCANNING PLATFORM

In order to perform a topographic survey in a time-efficient fashion, low-budget (compared to aerial LIDAR) and accurate way, a special service vehicle (SSV) with an innovative scanning system was developed at the Department of Geography of Ghent University, Belgium (fig. 2.1) (Incoul et al., 2014). It consists of a mobile platform (Kymco) equipped with a terrestrial laser scanner (TLS, Leica (Z&F) HDS6100, fig. 2.2A), a Real-Time Kinematic Global Navigation Satellite System (RTK GNSS, Septentrio AsterXu, fig. 2.2B) and an Inertial Motion Unit (IMU, Octans 3000, fig. 2.2 C) as main components, connected to a rugged PC running QINSY software. The combination of the INS and GNSS measurements by the Position and Orientation measurement System (POS) provide highly accurate positioning. At the same time the laser scanner produces a very precise and dense point cloud.

Next to the measurement of (x,y,z)-coordinates by the laser scanner, an intensity value (*I*) is registered for each point (Stal, et al., 2014). This value represents the received backscatter of the emitted signal and is theoretically described by the laser range equation (Kaasalainen et al., 2011).
The main goal of this surveys is the construction of DSMs with high resolution and high accuracy. Furthermore, considering the return of the backscatter value for each measured point, provisional analysis of these values suggests a relation between the physical properties of the reflecting surface and the registered backscatter values. The quality of the DSMs of the laser scanning techniques (MTLS and STLS) is limited by various factors, specifically related to the beach environment (Barber et al., 2008). For instance, the humidity of the sand plays an essential role in the accuracy of the acquired DSMs. It has been demonstrated that the sand moisture is one of the components, besides grain size, that defines the reflectance parameter. As the sand properties of the Belgian beaches are identical on the intertidal area, the grain size diameter is a constant parameter: about 0.2 mm grain size or 'Well sorted very fine sand' according to the Gradistat method (Blott & Pye, 2001).

Figure 2.1. Leica (Z&F) HDS 6100 phase scanner (left) mounted on the special service vehicle (right)

This way, dense point clouds (hundreds of points per square meter) are attained with millimeter accuracy in a small time span: a section of 250 m by 250 m can be scanned in an orthogonal pattern with 20 m path intervals in less than one hour. Typically, the mobile platform speed is kept constant at 2 m/s (7,2 km/h) and 20 cross-sections per second are scanned, yielding a cross-section interval distance of 10 cm. In the cross-section profile direction, a point is measured every 0,074 degrees, corresponding with approximately 2000 points in a cross-section profile with a linear interval distance between 0.7 and 7 cm.

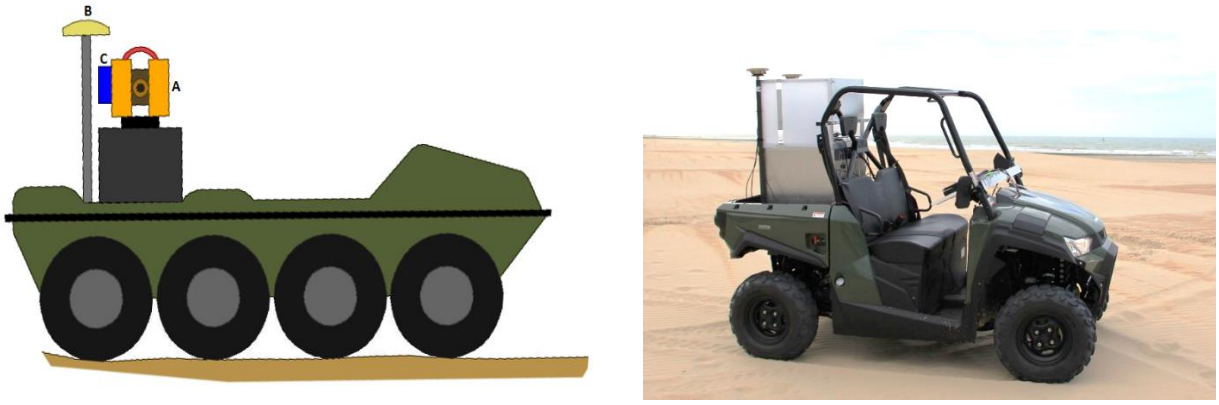

Figure 2.2. Mobile scanning platform: concept (left) and implementation (right)

3. FILTER ALGORITHM

Point clouds of backscatter based laser scanning surveys always contain a certain amount of false surface points ("noise"). In the context of the *SeArch* project (www.sea-arch.be) the Department of Geography of Ghent University developed an algorithm to eliminate these false surface points for LiDAR surveys of sandy beach surfaces. As it is of the utmost importance that micro-ripples can be distinguished both as an indication of sub-bottom anomalies and as an indication of morphological

sand dynamics, the algorithm has to be accurate: a filter which is too aggressive will smooth the surface, resulting in the disappearance of the existent micro-ripples. On the other hand, a filter which is too mild will result in a point cloud with non-surface points. This paper elaborates on the concept and implementation of the noise reduction algorithm.

3.1 Procedure Overview

The newly developed algorithm consists of several modules (Figure 3.1). This section describes the working of each module in detail. The algorithm allows the processing of mobile (MTLS) LIDAR surveys.

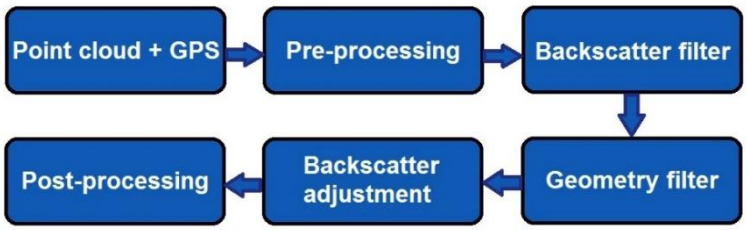

Figure 3.1: Overview of the algorithm's modules.

The minimal content requirement for the point cloud file is that each point of the cloud is specified by its three Cartesian coordinates and the backscatter value, needed for the backscatter based filter module. Other parameters might also be included, but they won't affect the algorithm. A separate file containing the RTK-GNSS trajectory includes for every time step of 0,1 s three Cartesian coordinates. For the MTLS measurements a piecewise linear connection will result in the approximate trajectory of the vehicle. The application of GNSS coordinates is useful for the subdivision of the cloud into smaller segments and for the adjustment of backscatter values in function of the distance between laser scanner and target.

3.2 Pre-processing

First, the global point cloud is geometrically transformed in a way that it can be subdivided into smaller segments. This has the advantage that the distance to the laser can be calculated and that geometrical and backscatter based outliers can be removed in an efficient way. For point clouds resulting from a mobile survey, the subdivision will be based on the line segments between two subsequent RTK-GNSS points: by rotating a RTK-GNSS segment such that it coincides with the x axis, data points with an x coordinate lying between the end points of this line segment, belong to the same cloud segment. Since each cloud segment has to contain a sufficient number of data points to get statistically significant results, GNSS points lying too close to one another are removed. Here, the criterion for removal is set to a minimal distance of 0.15 m between two subsequent RTK-GNSS points This threshold value is related to the driving speed of 2 m/s and the 10 Hz acquisition speed of the RTK-GNSS, yielding an average RTK-GNSS segment length of 20 cm.

The Belgian coast has a relatively homogeneous relief with typical height differences in the order of 4-5 m over a sand beach distance of approximately 300 m, yielding inclinations of a bit less than 1

degree or around 1.5 %. Height outliers, originate e.g. from levitating sand grains, should be removed from the cloud. First, a 3D translation over the centre of the point cloud is performed. After applying the translation, two rotations around the planar axes (*x* and *y* axes) are executed in order to minimize the global inclination of the. The removal of height outliers is based on a classical boxplot outlier test. After sorting the algebraic height values from low to high, and with the first and third quartile represented by respectively Q_1 (25 % of the data is lower) and Q_3 (75 % of the data is lower) and the height interquartile range (Q_3-Q_1) by *IQR*, the height outlier condition is given by both inequalities:

$$Q_1 - z_i > Q_f \,.\, IQR \quad \text{and} \quad z_i\text{-}Q_3 > Q_f \,.\, IQR \tag{3.1}$$

where Q_f is set to 1,5 and z_i is the height coordinate of cloud point *i*. After the outlier elimination, the point cloud is restored in its original location by performing the inverse rotations and inverse shift.

As mentioned before, the subdivision of the point cloud is based on the several GNSS line segments. Line segment is formed by the vectors $\overrightarrow{GNSS_k}$ and $\overrightarrow{GNSS_{k+1}}$, where $\overrightarrow{GNSS_k}$ is built from the three Cartesian coordinates of GNSS point *k*. First, the cloud is shifted over GPS_k.

$$\overrightarrow{V_k} = \overrightarrow{GPS_{k+1}} - \overrightarrow{GPS_k} \tag{3.2}$$

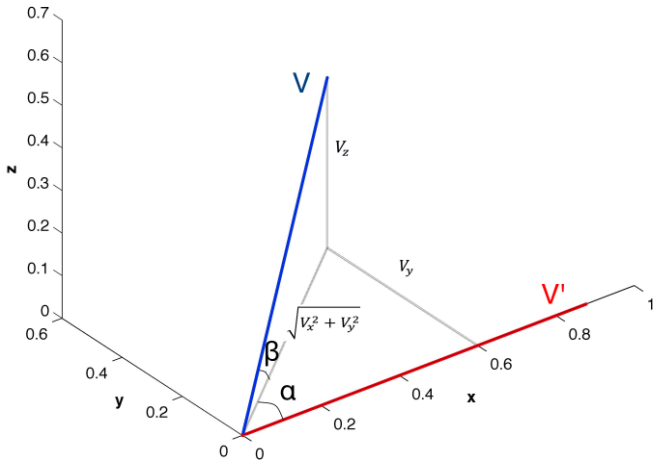

Figure 3.2: Definition of the rotation angles α_k and β_k and line segments $\overrightarrow{V_k}$ and $\overrightarrow{V'_k}$

Next, two rotations are performed, in a way that $\overrightarrow{V_k}$ (eq. 3.2) coincides with the *x* axis. The two rotation angles α_k and β_k are defined as (Figure 3.2):

$$\alpha_k = -\arctan\left(\frac{V_{k,y}}{V_{k,x}}\right) \tag{3.3}$$

$$\beta_k = \arctan\left(\frac{V_{k,z}}{\sqrt{V_{k,x}^2 + V_{k,y}^2}}\right) \tag{3.4}$$

Finally, all points with an x-coordinate between 0 and the length of segment $\overrightarrow{V_k}$ are selected. In this way, cloud points having a negative *x* coordinate, belonging to line segments 1 to *k*-1 are not taken into account. The same is valid for points belonging to line segments k+1 and higher, where the x-coordinate is bigger than the segment length $\overrightarrow{V_k}$.

Since the GNSS trajectory between GNSS points *k* and *k*+1 is parallel to the *x* axis, the distance *R* between laser scanner and target *l* can easily be calculated as:

$$R = \sqrt{y_l^2 + z_l^2} \tag{3.5}$$

3.3 Backscatter filter

It is well known that backscatter is dependent on both physical and non-physical parameters. Examples of physical dependencies are the humidity and grain size of the reflecting (sandy) surface). The influence of the radial distance *R* between laser scanner and target and the incidence angle of the reflector are non-physical dependencies.

Typically, the backscatter values decrease with the slope distance at both sides of the mobile platform. This is due to multiple factors, but the most important ones are the increasing laser beam width, and the decreasing angle between the laser beam and beach surface.

Both a logarithmic and an exponential and model were considered to model the backscatter

- *I* is logarithmically dependent on *R*. The linear fit is performed on:

$$I = a + b \ln R \tag{3.6}$$

- An exponential model, where a linear fit is executed on $ln\, I = a + b\, R$ with *a* and *b* fit parameters. This results, with $a' = e^a$, in:

$$I = a' e^{bR} \tag{3.7}$$

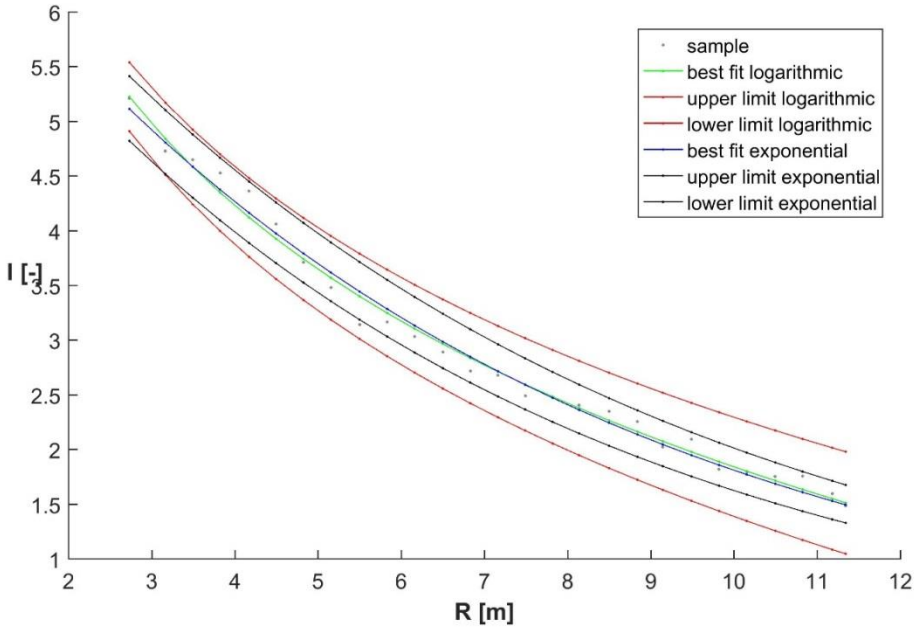

Figure 3.3: Comparison of the absolute backscatter variability between the exponential and logarithmic models.

The range of the intensity values can be adjusted in the acquisition software QINSY: the minimum value of the range was set to 5000 and the maximum value of the range to 5 million. The exponential model proved to be the optimal model for backscatter as a function of the radial distance R (figure 3.3), with typical approximate values of a and b of respectively 7.5 and -0,15. The determination coefficient R^2 is typically around 99 % and the fit parameter variability on a and b is around 5 %, what can be considered as a satisfying modelling of the sample intensity values, which are averaged for 0.2 m distance intervals to mitigate the effect of the higher laser point density close to the scanning platform.

While the logarithmic model includes the smallest relative variability in fit parameters, the exponential model has the smallest absolute backscatter variability; the distance between the two black curves is smaller than the distance between the two red ones (fig. 3.3).

The backscatter based filter parameters are computed and applied to each cloud segment separately. New backscatter values are determined by subtracting the best fit backscatter I_{fit} values from the original ones:

$$I_{new} = I - I_{fit} \tag{3.8}$$

This means that a new reference level for backscatter has been introduced, where the possible dependency on the distance is minimized. This readjustment is required, because the determination of backscatter outliers is based on a boxplot outlier test: if it wouldn't be readjusted, only backscatter values at the smallest and largest distances would be removed. After computation of the Q_1, Q_3 and IQR (=Q_3-Q_1) values of the sorted I_{new} distribution, Backscatter is considered as an outlier if:

$$Q_1 - I_{new,i} > Q_f \,.\, IQR \quad \text{and} \quad I_{new,i} - Q_3 > Q_f \,.\, IQR \tag{3.9}$$

where Q_f = 1.5 and consequently those data points are removed from the cloud. Finally, the backscatter values of the remaining data points are readjusted to their original values.

3.4 Geometry filter

The geometry based filter is based on local inclination outliers in each RTK-GNSS segment. First, the inclinations of each cloud segment are minimized using two rotations, based on a classical planar fit:

$$z = ax + by + c \tag{3.10}$$

Next, a Delaunay triangulation is performed. The edges of the triangles relate neighbouring data points, allowing to compare the local inclination k (corresponding to the edge E_k) between two points p_i and p_j (Fig. 3.4):

$$\gamma_k = \arctan\left(\frac{\left|p_{i,z} - p_{j,z}\right|}{\sqrt{\left(p_{i,x} - p_{j,x}\right)^2 + \left(p_{i,y} - p_{j,y}\right)^2}}\right) \tag{3.11}$$

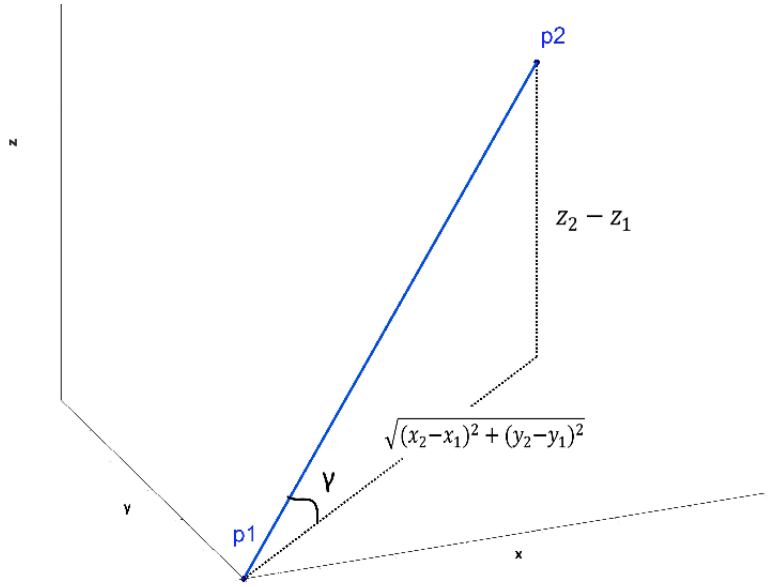

Figure 3.4: Computation of the local incidence angle

As seen in eq. (3.11), γ_k is defined to be positive. Without taking the modulus of $(p_{i,z} - p_{j,z})$ the slope γ_k would be dependent on the order of p_i and p_j, and the result would be dependent on the order of points in the triangulation, which is undesirable.

After computation of the Q_3 and IQR (=Q_3-Q_1) values of the sorted γ_k distribution, the outlier condition for γ_k is stated as:

$$\gamma_k - Q_3 > Q_f \cdot IQR \qquad (3.12)$$

where Q_f is a quality factor set to 1.5. This quality factor should be carefully chosen: the key point of the geometric outlier test is to eliminate points about the beach surface (due to wind transported sand particles, people, animals or obstacles on the beach,…) but to keep the surface relief as this is the indicator of possible subbottom areacheological findings or geomorphologic sand ribble dynamics. If the value of Q_f is excessive, valuable surface relief information is lost, and a smaller Q_f should imperatively be used.

The interval of acceptance has only an upper limit, because the minimum value of γ_k is equal to zero. Next, for each outlier of γ_k the endpoints of the corresponding edge E_k are considered. To decide which one of the two is an outlier, the numbers of inclination outliers corresponding to the edges attached to these points are considered. If e.g. p_i has more corresponding γ_k outliers than p_j, it is more plausible that p_i is the outlier instead of p_j. If their numbers are equal, the data point with the largest z coordinate is seen as outlier, because height outliers usually lie above the scanned surface.

Finally, two inverse rotations return the cloud segment to its original orientation. The minimum and maximum inclination values γ_k of the edges of each point, connected to its neighbours, is also kept

and written to the resulting point cloud file to allow further interpretation in the post-processing module.

3.5 Backscatter adjustment

Intensity maps are able to visualise the morphology of sandy beach structures. Since different inclination angles correlate to morphological variations, their effect on backscatter is kept, but the distance influence must be corrected. Backscatter values of the resulting filtered point cloud can be adjusted using equation 3.8. This way, and quite similar to the backscatter filter module (cf. 3.3), the backscatter value of all points are adjusted using an exponential correction model. However, by recomputing the correction parameters a and b (equation 3.7) for the point cloud reduced by the geometric filtering (cf. 3.4), a finer backscatter correction can be achieved. The optimal a and b values are computed for each RTK-GNSS segment independently, as it can be expected that local variations in humidity and (sun)light conditions could have a significant impact on the boxplot outlier test used in the backscatter filter module. The corrected I_{new} values of each point are written to the resulting point cloud file to allow further interpretation in the post-processing module.

3.6 Post-processing

The final module performs the inverse translations and rotations of the ones specified in the pre-processing. It also glues the different cloud segments to one global, exported, point cloud. As for each point, the corrected backscatter value and minimum/maximum slope values were also saved, further analysis based on these combined values can be performed, as typical sand ripples will exhibit a correlation between a backscatter irregularity and a slope irregularity. Choosing adequate visualisation colours for both values allows to identify the areas to further investigate either for sub-bottom relicts (cf. Search project) or for sand ripple morphologic dynamics (cf. Crest project). Hereunder, a geometric cross-section interpolated in the filtered model is presented (figure 3.5). The sand ripple structure is clearly discerned.

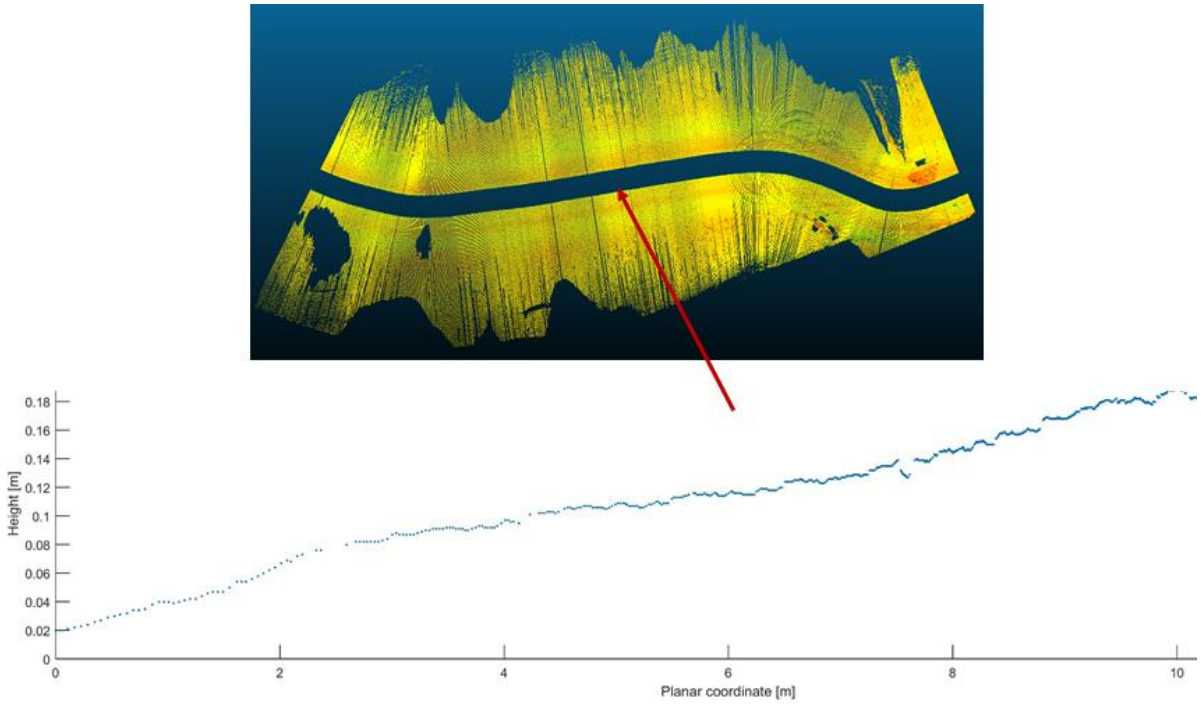

Figure 3.5: Example of a filtered cross-section of the beach .

4. CONCLUSION

A concept of a noise filter algorithm for a mobile scanning platform, developed for sandy beaches, was presented. The presented noise reduction procedure appears to be very effective for both the noise elimination as for the extraction of the micro-relief features.

The presented procedure was validated using data of a test side in Raversijde (Belgium), and proved to provide a valid procedure to automatically remove measurement noise and false beach surface points.

However, the resulting filtered data point cloud isn't the endpoint, but, on the contrary, an ideal start point for further research of sand beach morphologic dynamics, based, on the one hand, on the study of the geometrical characteristics (slope differences), and, on the other hand, on the analysis of the variation of backscatter values.

In future research, supplementary algorithms are planned to be developed to automatically extract the movement of transversal and longitudinal sand ripples.

REFERENCES

Kaasalainen, S., Jaakkola, A., Kaasalainen, M., Krooks, A., Kukko, A. (2011) Analysis of incidence angle and distanceeffects on terrestrial laser scanner intensity: Search for correction methods. *Remote Sensing*, 3:2207-2221.

Barber, D., J. Mills & Smith-Voysey, S. (2008) Geometric validation of a ground-based mobile laser scanning system. *ISPRS Journal of Photogrammetry and Remote Sensing*, 63, 128-141.

Blott SJ, Pye K. (2001) Technical Communication Gradistat : a Grain Size Distribution and Statistics Package for the Analysis of Unconsolidated Sediments; 1248: 1237–48.

De Wulf, A., De Maeyer, P., Incoul, A., Nuttens, T., & Stal, C. (2014). Feasibility study of the use of bathymetric surface modelling techniques for intertidal zones of beaches. *Proceedings (FIG International Congress)*. Presented at the 25th FIG Congress: Engaging the challenges, enhancing the relevance, International Federation of Surveyors (FIG).

Incoul, A., Nuttens, T., De Maeyer, P., Seube, N., Stal, C., Touzé T. , De Wulf, A. (2014) Mobile laser scanning of intertidal zones of beaches using an amphibious vehicle. In *6th International conference on Engineering Surveying* (INGEO 2014), 87-92. Slovenská Technická Univerzita v Bratislave. Stavebná Fakulta.

Middleton, J., Cooke, C., Kearney, E., Mumford, P., Mole, M., Nippard, G., Rizos, C., Splinter, K., Turner, I. (2013) Resolution and accuracy of an airborne scanning laser system for beach surveys. *Journal of Atmospheric and Oceanic Technology*, 30, 2452-2464.

Stal, C., Incoul, A., De Maeyer, P., Deruyter, G., Nuttens, T., De Wulf, A. (2014) Mobile mapping and the use of backscatter data for the modelling of intertidal zones of beaches. In *14th SGEM GeoConference on Informatics, Geoinformatics and Remote Sensing*, 223-230. Stef92 Technology.

White, S. A., Parrish, C. E., Calder, Pe'eri, B.R., Azhanov, R. (2011) LIDAR-Derived National Shoreline: Empirical and Stochastic Uncertainty Analyses. *Journal of Coastal Research*, 62, 62-74.

BIOGRAPHICAL NOTES

Prof. dr. ir. Alain De Wulf is full-time professor at Ghent University (Belgium), researching and lecturing on the general principles of 3D data-acquisition techniques in the domains of land and hydrographic surveying and quality aspects of geodesy in particular. He is vice-chairman and secretary of the Hydrographic Society Benelux.

With his expertise in hydrographic surveying, he is developing specialized software for the processing and quality assessment of hydrographic data acquisition sensors.

He was and is involved with his scientific research team in different projects, ranging from topographic campaigns for archaeological projects (Malta, Altai (Russia), Thorikos, Titani (Greece), etc.) to bathymetric projects involving vertical reference surfaces and GNSS buoy tide measurements. In these projects, recent developments in surveying engineering, photogrammetry, bathymetry and geomatics are actively applied in state-of-the-art and integrated 3D data acquisition techniques and platforms.

CONTACTS

Prof.dr.ir. Alain DE WULF
Ghent University – Department of Geography
Krijgslaan 281, Building S8
9000 Ghent
BELGIUM
Tel. +32 9 264 46 56
Fax. +32 9 264 49 85
Email: Alain.DeWulf@ugent.be
Web site: http://geoweb.ugent.be/3dda